Stacked H-Shaped Microstrip Patch Antenna

Jaume Anguera, *Member, IEEE*, Lluís Boada, Carles Puente, *Member, IEEE*, Carmen Borja, *Member, IEEE*, and Jordi Soler, *Member, IEEE*

***Abstract*—A small H-shaped microstrip patch antenna (MPA) with enhanced bandwidth is presented. The H-shaped antenna is first studied by a transmission line model and then is fully analyzed with a MoM code. A stacked patch configuration is proposed to increase the narrow bandwidth, radiation efficiency and directivity. The stacked H-shaped MPA is studied using Chu's fundamental limit for electrically small antennas.**

***Index Terms*—H-shaped antennas, limit of Chu, microstrip antennas, small antennas, stacked patches.**

I. Introduction

MINIATURIZATION of microstrip patch antennas (MPAs) is a very challenging field to investigate due to the increasing interest in integrating such antennas in MMIC circuits. The conventional dimensions of MPAs are around a half waveguide wavelength. Several miniaturization techniques are appearing to reduce such dimensions. These techniques can be classified in: 1) use of high permittivity substrates; 2) use of magnetic substrates; 3) increase electrical length; 4) short-circuits; 5) superstrates and 6) combinations of them [1].

Using high permittivity substrates, the antenna size can be considerably reduced. One of the main problems is the surface-wave mode excitation causing a reduction of surface-wave radiation efficiency. Moreover, as the substrate has finite dimensions, the diffracted field due to the surface-wave mode, degrades the radiation pattern increasing the side-lobe level and increasing also the crosspolar field. In arrays, the mutual coupling caused by surface wave modes limitates beam-steering. One recent technique to overcome these problems is the use of electromagnetic band gap (EBG) substrates [2].

Magnetic substrates can reduce antenna size with a wider bandwidth with respect to dielectric substrates. However, it is unlikely to obtain pure magnetic material and some preliminary attempts are trying to simulate them using lattices of loaded loops [3].

Increasing electrical length technique consists in perturbing strategically the patch surface. Between these perturbations, the square and circular rings are well-known alternatives to obtain small patches when compared to the filled versions [4]. Other well documented geometries are the H-shaped and meander patches [5], [6]. One novel geometry is inspired in fractal shapes. An example of a miniature MPA based on the Sierpinski fractal is presented in [7], [8].

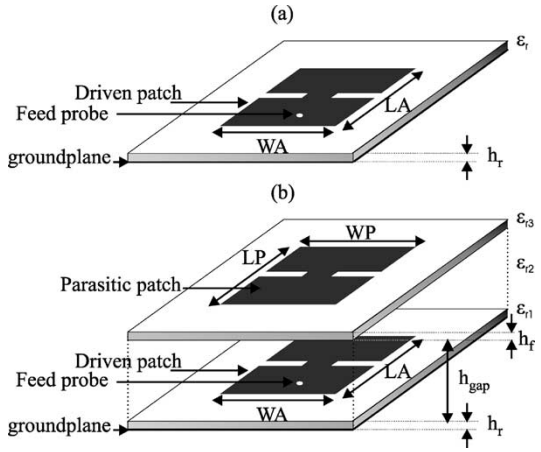

Fig. 1. a) Single patch configuration and b) stacked configuration.

Short-circuited patch techniques consist in shorting the surface patch to the ground plane and such that the antenna can resonate at a quarter waveguide wavelength. This size reduction is accompanied by reduced gain, high cross-polarization in H plane and also a high tolerance for the feed position which becomes a main problem concerned with the fabrication process [9].

The utilization of superstrates enables a size reduction caused by a modification of the effective dielectric constant. A significant increase of gain and efficiency can be achieved. The superstrate acts two-fold: protects the antenna against environmental conditions, e.g., ice, rain, and improve electrical behavior [10].

Combination of the above mentioned techniques can be used to mix their advantages [11].

A common problem related with miniature antennas is the narrow bandwidth (BW) and poor radiation efficiency [12]. In this paper, we will investigate the H-shaped MPA as a miniature antenna and how to increase the bandwidth and radiation efficiency. To achieve this goal, a stacked patch with H-shaped geometry is proposed (Fig. 1). Sections II and III present an electrical network based on the transmission line model to predict the change of resonant frequency as a function of the H-shaped geometry. In Section IV, several H-shaped MPAs are characterized using a conventional MoM code. The numerical data is then contrasted with experimental results. In Section V, the parasitic patch solution is analyzed. Several prototypes are presented. In Section VI, the antennas are analyzed using the Chu's fundamental limit on electrically small antennas. Finally, Section VII summarizes and concludes the work.

Manuscript received September 3, 2001; revised May 12, 2003. This work was supported by Fractus.

J. Anguera was with the Technology Department, Fractus S.A., 08190, Barcelona, Spain. He is now with Technology Department, Fractus-Korea, Kyunggi-Do, 463-828 Korea (e-mail: jaume.anguera@fractus.com).

L. Boada, C. Puente, C. Borja, and J. Soler are with the Technology Department, Fractus S.A., 08190, Barcelona, Spain.

Digital Object Identifier 10.1109/TAP.2004.825812

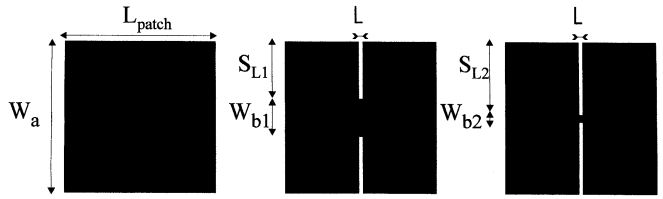

Fig. 2. Metamorphosing the square patch to H-shaped patch.

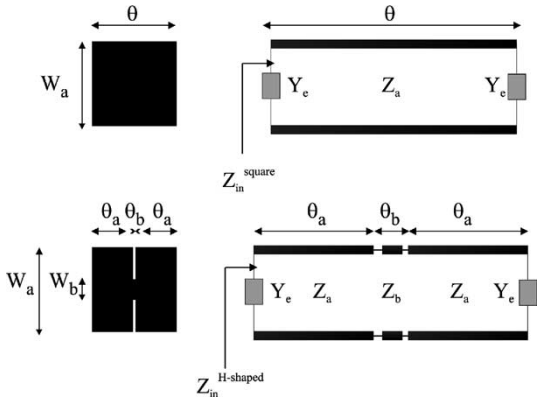

Fig. 3. Transmission line models for the square and H-shaped patch antennas.

II. Transmission Line Model

The transmission line model has been extensively used to predict the input impedance, resonant frequencies and bandwidth of square patches [13]. In this section, the transmission line model is used to study the resonant frequency of the H-shaped patch as a function of the slot dimensions (Fig. 2).

Fig. 3 shows the proposed transmission line model for the square and H-shaped MPAs. The length of the square patch is designed by the electrical length θ while the H-shaped length is designed by two sections of θ_a and one section of electrical length θ_b. The transmission-line characteristic impedances are denoted by Z_a and Z_b depending of the transmission line width W_a and W_b, respectively (Figs. 2 and 3). Y_e is the admittance that takes into account the radiating slots.

If the square patch is designed to operate at the fundamental model (TM_{10}), then $\theta = \pi$ at $\mathrm{f} = f_o$, where f_o is the fundamental resonant frequency.

Controlling Z_b and θ_b it is possible to decrease the resonant frequency. Assuming the width W_b is small and $\theta_b \ll \pi$, the transmission line (Z_b, θ_b) of Fig. 3 can be approximated by an inductance L. Therefore, the H-shaped antenna transmission line model of Fig. 3 is converted to Fig. 4. Now, $2 \cdot \theta_a \approx \theta$. In Fig. 4, Y_e has been neglected to simplify the model and to study the frequency variation as a function of the slot itself. The slot capacitance effect is also neglected in this first model. In the second model (Section III) the slot capacitance effect is taken into consideration. This way, one can study the frequency relations as a function of the transmission line junction and then as a function of the slot capacitance effect.

As the goal is to achieve a miniature antenna, the input impedance of Fig. 4 is forced to be the same of a transmission line with characteristic impedance Z_a and electrical length $\theta' > \theta$ (Fig. 5).

A miniaturization parameter g is introduced. This g is defined as a shifting frequency factor as: $\theta' = \pi$ at $f = g \cdot f_o$. The

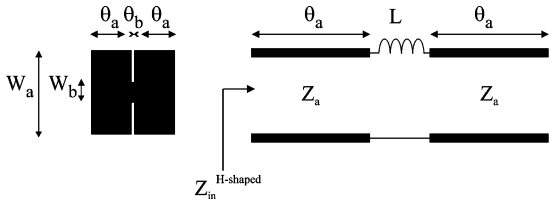

Fig. 4. Simplified transmission line model for the H-shaped MPA.

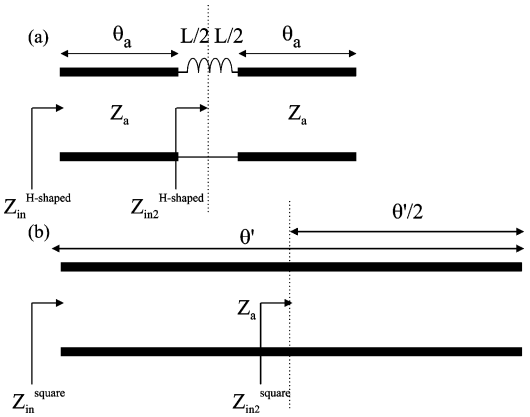

Fig. 5. a) Simplified transmission line model for the H-shaped MPA. b) Transmission line that resonates at the same frequency as the transmission line circuit of a).

range of g is [0, 1]. Thus, by equating $Z_{\mathrm{in2}}^{\mathrm{square}}$ to $Z_{\mathrm{in2}}^{\mathrm{H-shaped}}$ of Fig. 5 an equation relating L with the miniaturization factor g can be extracted. As L is related to Z_b and W_b, a design equation relating the H-shaped geometry with the resonant frequency can be deduced. Taking into consideration the circuit symmetry, the process is detailed as follows:

$$Z_{\mathrm{in2}}^{\mathrm{H-shaped}} = \frac{j2\pi f L}{2} - jZ_a \cot(\theta_a) \tag{1}$$

$$Z_{\mathrm{in2}}^{\mathrm{Square}} = -jZ_a \cot\left(\frac{\theta'}{2}\right) \tag{2}$$

$$Z_{\mathrm{in2}}^{\mathrm{H-shaped}} = Z_{\mathrm{in2}}^{\mathrm{Square}} \tag{3}$$

$$L = \frac{2Z_a\left[\cot(\theta_a) - \cot\left(\frac{\theta'}{2}\right)\right]}{2\pi f}. \tag{4}$$

As we are concerned in searching for the value L that allows circuit of Fig. 5(a) to resonate at $g \cdot f_o$, in (4) f is assumed to be $g \cdot f_o$, i.e., $f = g \cdot f_o$

$$L = \frac{2Z_a\left[\cot(\theta_a) - \cot\left(\frac{\theta'}{2}\right)\right]}{2\pi g f_o}. \tag{5}$$

As $\theta_b \ll \pi$, then $2\,\theta_a \simeq \pi$ at $f = f_o$; then

$$\theta_a \simeq \frac{g \cdot \pi}{2} \;\; at \;\; f = g \cdot f_o. \tag{6}$$

As

$$\theta' = \pi \;\; at \;\; f = g \cdot f_o \tag{7}$$

then

$$L = \frac{2Z_a \cot(\theta_a)}{2\pi g f_o} = \frac{2Z_a \cot\left(\frac{g\pi}{2}\right)}{2\pi g f_o 0}. \tag{8}$$

If the inductance $\mathrm{L} = 0$, then $\mathrm{g} = 1$ as expected. If $\mathrm{L} \to \infty$, then $\mathrm{g} \to 0$. Thus, by controlling L, the resonant frequency

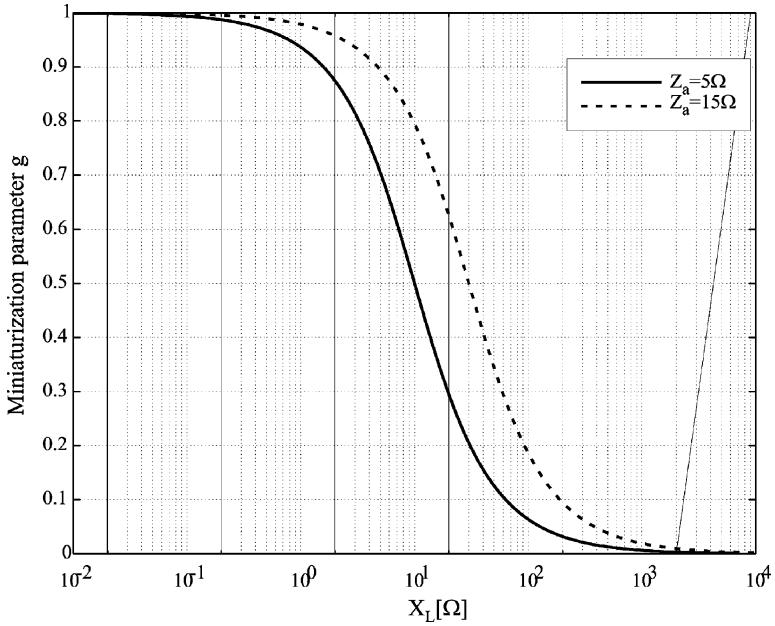

Fig. 6. Miniaturization parameter g as a function of reactance X_L.

of the H-shaped patch antenna can be adjusted. It is interesting to outline the nonlinear dependence between L and g (8). The reactance associated to L is easily calculated as follows:

$$X_L = 2 \cdot \pi \cdot g \cdot f_o \cdot L = 2 \cdot Z_a \cdot \cot \frac{g\pi}{2}. \tag{9}$$

Fig. 6 represents (9) for two different values of Z_a.

From Fig. 6, it is relevant to see that for a certain range of the reactance X_L, the frequency can be shifted downwards and thus a miniature antenna is obtained. Moreover, for a given reactance, the resonance frequency can be also decreased by controlling the width (W_a) of the H-arms (Fig. 2) which determine Z_a.

The next step is to relate L with its physical counterparts: θ_b and Z_b. This relation is based on the inductance approximation of a short and high impedance transmission line [14]. The process is straight forward and results in

$$L \simeq \frac{Z_b \cdot l \cdot \sqrt{\varepsilon_r}}{c} \tag{10}$$

where l is the length of the short transmission line defined in Fig. 2.

To summarize the design process an example of a 2 GHz patch is converted to a H-shaped patch to resonate at 1.5 GHz. Then, the miniaturization factor $g = 1.5/2$. If the square patch is etched on a $h = 1.52$ mm and $\varepsilon_r = 3.38$ substrate, the dimensions are easily calculated resulting $W = L = 40$ mm. With this values, $Z_a = 7\ \Omega$. Finally L is calculated though (9) resulting $L = 0.6$ nH. Using the short transmission line approximation, $l = 2$ mm and $Z_b = 50\ \Omega$ ($W_b = 3.5$ mm).

III. Improved Transmission Line Model

The transmission line model of Fig. 4 can be improved if a capacitance effect is taken into account as shown in Fig. 7(a) and (b). Fig. 7(a) shows a capacitive π-network based on the microstrip gap discontinuity approaches [15]. The C_p capacitance has been neglected [Fig. 7(b)] because the patch is electrically near from the groundplane and only C_g is taken into consideration.

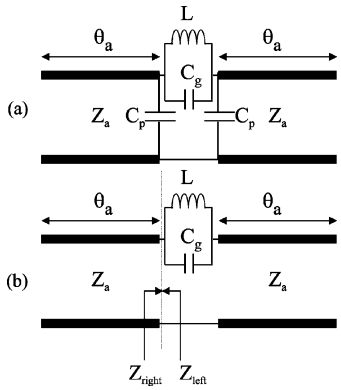

Fig. 7. a) Improved transmission line model considering a capacitance effect between the H arms. b) Simplified Improved transmission line model.

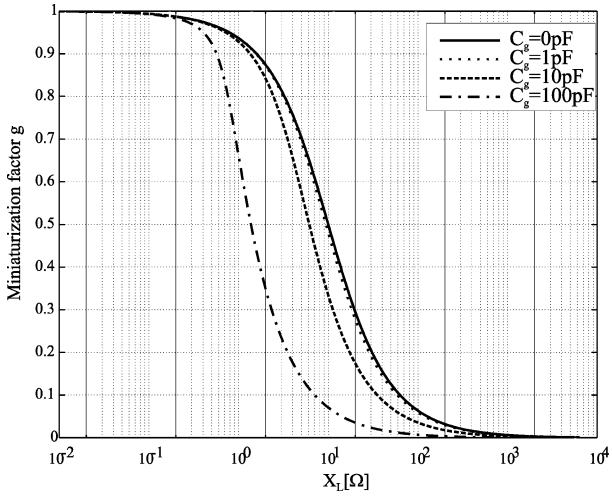

Fig. 8. Miniaturization factor g considering the LC model. $Z_a = 5\ \Omega$, $f_o = 2$ GHz.

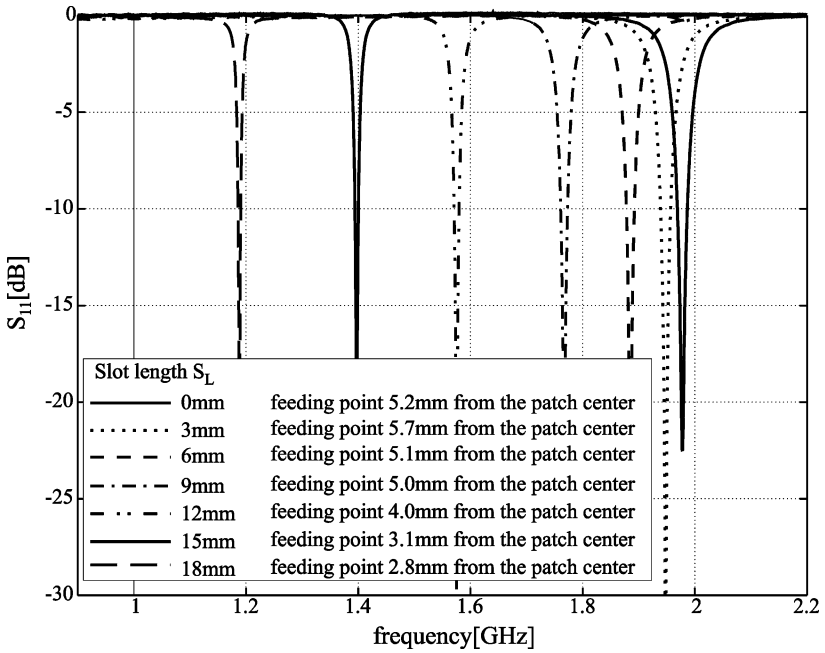

Fig. 9. Measured return loss as a function of the slot length.

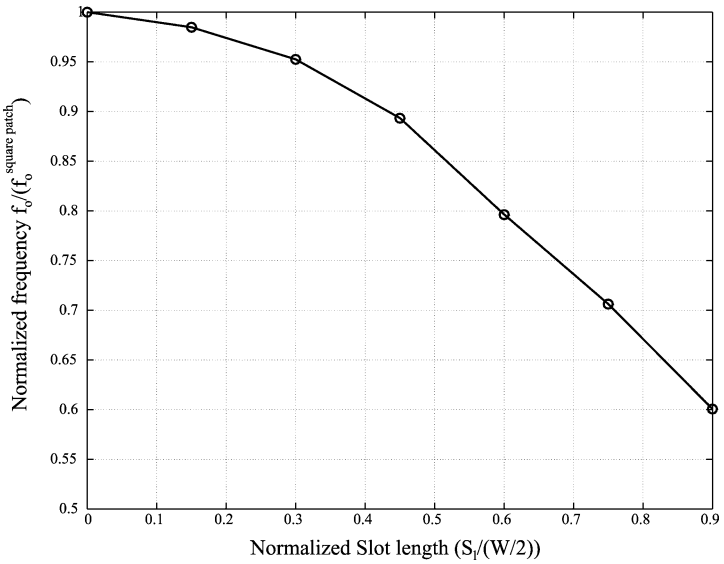

Fig. 10. Frequency reduction as a function of slot length.

TABLE I
RESONANT FREQUENCY, BANDWIDTH, QUALITY FACTOR AND ELECTRICAL SIZE. S_L = Slot Length, Q = Quality Factor, ES = Electrical Size.

S_L[mm]	$f_o[GHz]$	$BW[\%, SWR = 2]$	Q	ES [λ]
0	1.978	1.12	63	0.264
3	1.948	0.92	77	0.260
6	1.884	0.79	89	0.251
9	1.767	0.73	97	0.236
12	1.575	0.50	141	0.210
15	1.397	0.43	164	0.186
18	1.188	0.42	168	0.158

Depending on the slot length (S_L), slot width(l) (Fig. 2) and permittivity of the substrate where the patch is etched, the capacitance associated with the slot changes. Closed expressions can be found from the formulas for even and odd mode capacitances of coupled microstrip lines [15]. This gap discontinuity is useful in the design of gap-coupled microstrip antennas [16], [17].

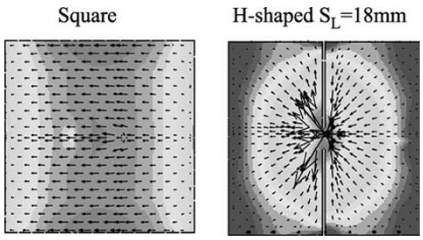

Fig. 11. Electrical current on the patch surface.

Applying the resonant condition $Z_{\text{left}} + Z_{\text{right}} = 0$ and considering (7), the reactance X_L of (9) results in

$$X_L = \frac{2Z_a \cot\frac{g\pi}{2}}{1 + 2Z_a \cot\frac{g\pi}{2} Y_C} \tag{11}$$

$$Y_C = 2\pi f_o g C_g. \tag{12}$$

Fig. 8 shows the variation of X_L versus the miniaturization factor g for several values of C_g. It shows that for a given X_L,

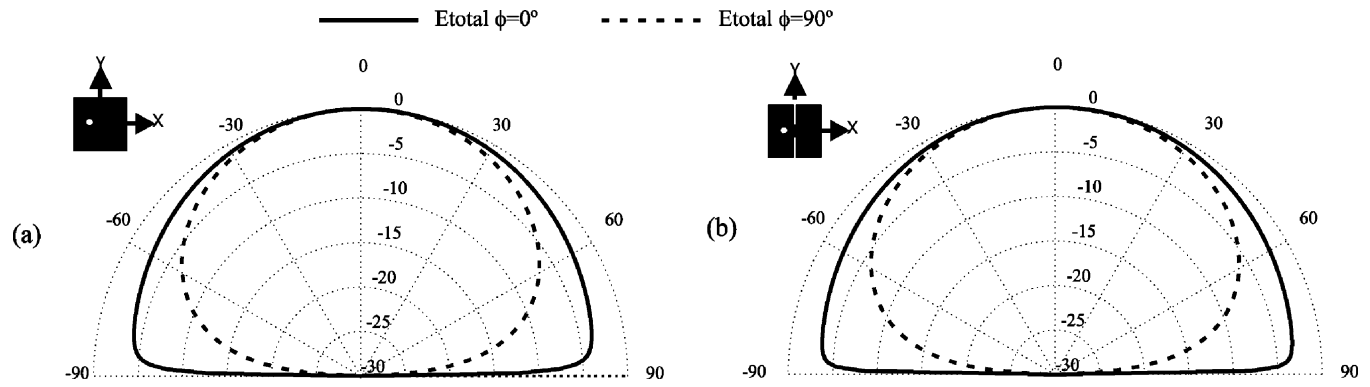

Fig. 12. Simulated radiation pattern: a) for the square patch at f $= 1.978$ GHz and b) for the H-shaped patch $S_L = 18$ mm at f $= 1.188$ GHz.

the antenna can be miniaturized further if the capacitance C_g increases.

The proposed transmission line gives a physical insight. By properly controlling the values of L(the transmission line length and width) and C_g(the slot length and width), the resonant frequency can be shifted downwards considerably. It is important to stress that the circuit models do not to pretend to predict exactly the resonant frequency but to know what variables allow to miniaturize the antenna. As a conclusion of the proposed transmission line model and presented equations we have the following.

1) If the inductance L increases, that is, if the transmission line is made narrower and longer (i.e., larger θ_b), the resonant frequency decreases.
2) If the coupling between H-arms increases, that is, if the slot S_L is made longer and thinner, the resonant frequency decreases.
3) If the characteristic impedance of H-arms Z_a decreases, that is, if the width W_a increases, the resonant frequency decreases. Obviously when increasing W_a, the slot length (S_L) also increases so a large frequency reduction can be expected when widening H-arms.

Following the concepts of these sections, several H-shaped patches are simulated and constructed to study the evolution of resonant frequency, the input impedance bandwidth, radiation efficiency, and directivity.

IV. Numerical and Experimental Results

Several H-shaped patches have been simulated with a MoM code and measured. The H-shaped patches are compared with the square patch. The original square patch is a 40×40 mm etched on a substrate with 1.52 mm height, $\varepsilon_r = 3.38$, and $\tan\delta = 0.0001$. The patches are fed through a coaxial probe and are matched to 50 Ω. Dimensions of the H-shaped patches are: slot width $\mathrm{l} = 1$ mm for all H-shaped patches and slot lengths (S_L) are: 3, 6, 9, 12, 15, and 18 mm (Fig. 2).

The return losses of the analyzed patches are measured on a network analyzer. Fig. 9 shows the return loss as a function of the slot length. The resonant frequency is shifted from the 1.978 GHz for the square patch to 1.188 GHz for the 18 mm slot length H-shaped patch (Fig. 10). This frequency reduction is about 40% which is important for antenna applications where space is a constraint factor.

Table I summarizes some features of the analyzed antennas.

Table I shows how the bandwidth is reduced when the antenna becomes electrically smaller. This is a consequence of small antennas: when the volume filled by the antenna decreases, the antenna quality factor Q increases so the bandwidth decreases [12]. However, for a same volume not all the antennas have the same Q. If an antenna fills the volume efficiently (the present case is a planar antenna so it does not fill the radian sphere properly), the quality factor would be lower and then the bandwidth would be higher. Therefore, for a same volume, if the antenna fills it efficiently, the bandwidth would be improved. This is the objective of Sections V and VI.

To conclude the analysis, the radiation parameters (directivity and efficiency) are calculated as a function of slot length. Fig. 11 shows the electrical current distribution on the patch surface. The current distribution is a TM_{10} mode distribution so one expects a similar radiation pattern than that for the square patch. A current maximum is located in the center of the patch because the whole current flowing from one edge to the other passes only by the small junction. Both current distributions have a null area at the radiating edges. For the H-shaped patch, the equivalent electrical length is longer than that for the square patch. For this reason, the resonant frequency can be shifted to a lower value.

The radiation pattern is calculated through the current integration on the patch surface. The main radiation cuts (E and H planes) for the square and H-shaped (Slot $= 18$mm) are shown in Fig. 12. The radiation cuts are similar, even being the H-shaped a small antenna, so the directivity is almost the same (Table II).

As indicated in Table II, the radiation efficiency decreases as the antenna becomes electrically smaller. The IE3D MoM code computes radiation efficiency as

$$\eta = \frac{P_{\mathrm{rad}}}{P_{\mathrm{rad}} + P_c + P_d + P_{sw}} \tag{13}$$

where P_{rad} is the radiated power, P_c and P_d are the conductor and dielectric losses respectively and P_{sw} is the surface wave power.

For the present case (frequency $<$ 2 GHz), the dielectric losses have been neglected ($P_d = 0$). On the other hand, as the substrate is electrically thin and only the dominant surface mode propagates, i.e., TM_0, the surface wave power is also neglected. Then, the radiation efficiency can be approximated by

$$\eta \simeq \frac{R_{\mathrm{rad}}}{R_{\mathrm{rad}} + R_c} \tag{14}$$

TABLE II
DIRECTIVITY, RADIATION EFFICIENCY AND GAIN SIMULATIONS. CONDUCTIVITY $\sigma = 4.9 \cdot 10^7$ S/m

Sl[mm]	D[dB]	η[%]	Gain[dB]
0	6.66	86	6
3	6.63	85	5.9
6	6.58	83	5.7
9	6.51	75	5.3
12	6.44	67	4.7
15	6.37	49	3.2
18	6.31	23	-0.07

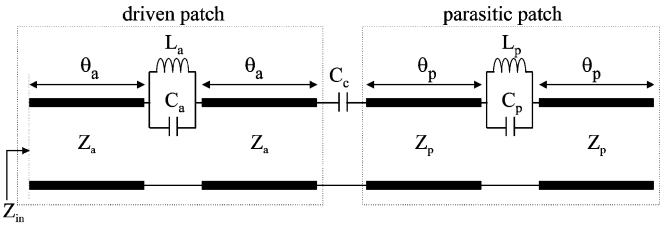

Fig. 13. Electrical model for the stacked structure of Fig. 1.

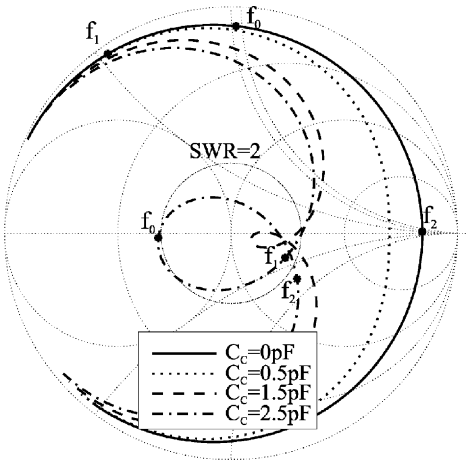

Fig. 14. Input impedance evolution for different values of the coupling capacitor C_C.$2\theta_a = 2\theta_b = \pi$ at 2 GHz. $Z_a = Z_b = 7\ \Omega$. $Q_a = 100$, $Q_p = 15$. $L_a = L_p = 614\ pH$, $C_a = C_p = 0\ F$.

where $R_{\rm rad}$ and R_c are the radiation and conductor loss resistance, respectively.

Taking into consideration these approximations, the radiation efficiency decreases for two reasons: 1) the radiation resistance $R_{\rm rad}$ decreases as the H-shaped MPA becomes electrically smaller and 2) the R_c increases because the patch is electrically closer to the ground plane as the antenna becomes miniature.

The poor radiation efficiency can be overcame if a conductor with a higher conductivity is used to decrease R_c. This improvement can be achieved by using superconductors [18]. Obviously this improvement of radiation efficiency will led a smaller bandwidth. In the next section, a technologically easier method to increase the radiation efficiency and even improving the bandwidth is explained. It consists in stacking a miniature parasitic patch based on the H-shaped geometry.

V. BROADENING BANDWIDTH

As presented in Section IV, the BW($SWR < 2$) is only 0.4–1%. There are several techniques to improve the bandwidth as increasing the substrate height [21], lowering the dielectric

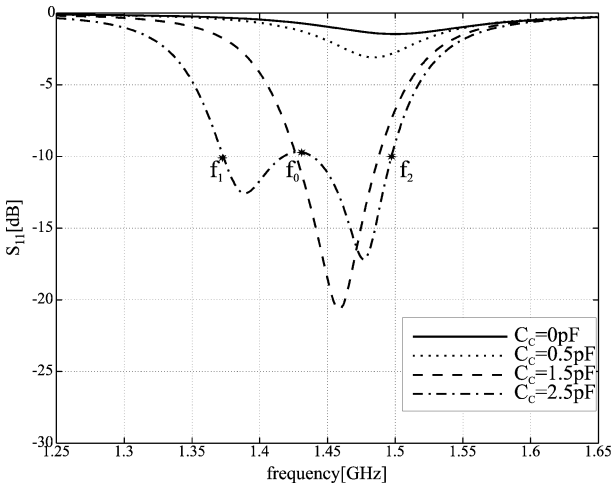

Fig. 15. Return loss for the simulation of Fig. 14.

TABLE III
DIMENSIONS OF THE STACKED PROTOTYPES

Parameter	$S_L = 15$	$S_L = 18$
W_A[mm]	40	40
L_A[mm]	40	40
S_{LA}[mm]	15	18
h_r[mm]	1.52	1.52
ε_{r1}	3.38	3.38
feeding point from MPA center[mm]	15	7.4
h_{gap}[mm]	16.5	11.9
ε_{r2}	1(air)	1(air)
W_P[mm]	59	59
L_P[mm]	59	59
S_{LP}[mm]	26	29
h_f[mm]	1	1
ε_{r3}	4.15	4.15
groundplane[mm^2]	80 × 80	80 × 80

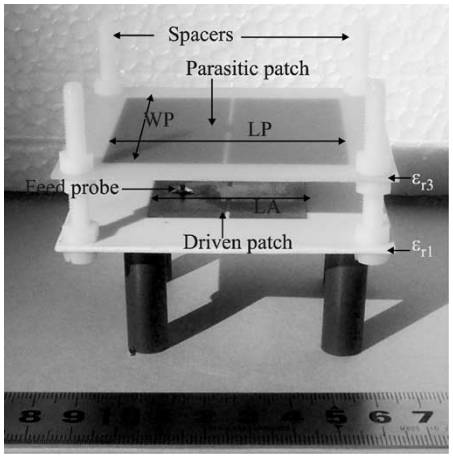

Fig. 16. Prototype of H-Shaped stacked antenna.

permittivity, using parasitic patches [19], broadband matching networks [20] and adding losses. In the present case, the solution of stacking a parasitic patch is chosen for several reasons: the bandwidth can be increased considerably, the radiation efficiency increases as well as directivity does. Fig. 1(b) shows the proposed stacked configuration.

The stacked configuration presents several design variables as the gap between patches, different dielectric permittivities,

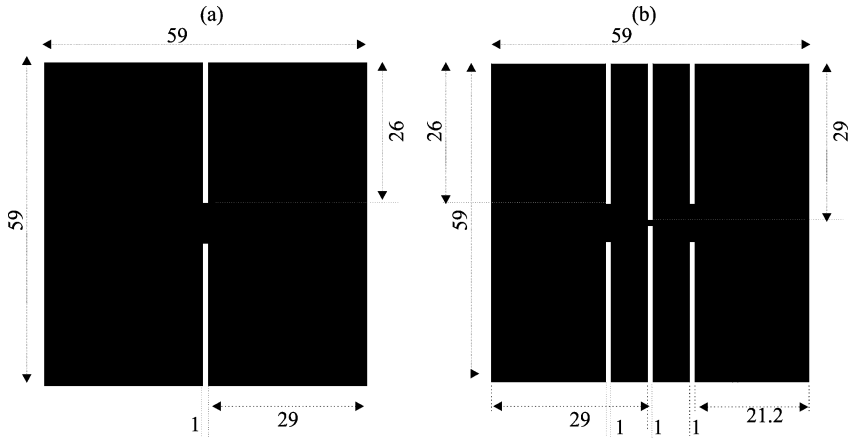

Fig. 17. Parasitic layouts. a) For the $S_{LA} = 15$ mm and b) for the $S_{LA} = 18$ mm prototypes.

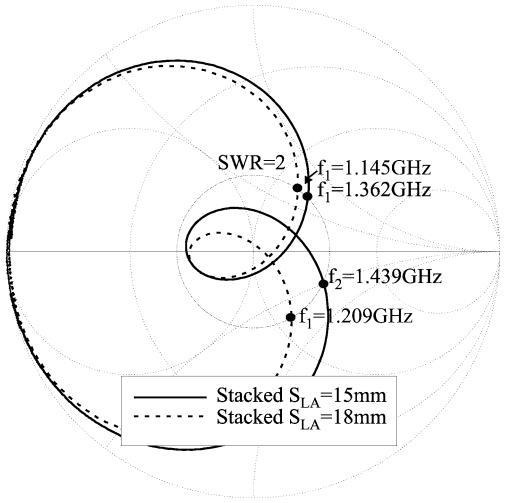

Fig. 18. Measured input impedance for the two stacked prototypes. First prototype has a driven patch with slot length of $S_{LA} = 15$ mm, and the second has a driven patch with slot length of $S_{LA} = 18$ mm.

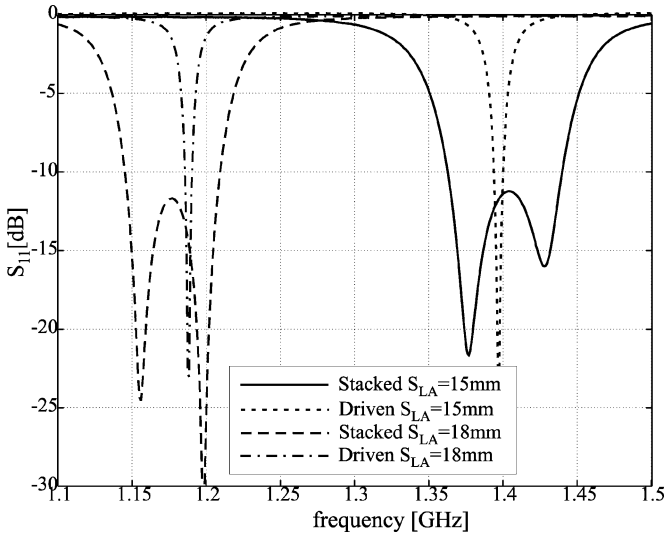

Fig. 19. Measured return loss for the stacked antennas compared with its belonging driven patch.

patch sizes and position of the feed probe. For this reason, the design of this structure is widely investigated. In this paper, the design rule presented in [19] has been used. In this case, the electrical model presented in [19] is modified as shown in Fig. 13.

The electrical model shown in Fig. 13 is useful for parametric analysis. First of all, if there is enough coupling between the driven and parasitic patches, an input impedance loop appears. The stronger the coupling is, the larger the size of the loop. Coupling is controlled by the gap between patches and it is represented in the model by the capacitor C_C. Secondly, the input impedance loop will be inductive if $f_p < f_a$ and viceversa being f_p and f_a the resonant frequencies of the parasitic and driven patches, respectively [19].

Fig. 14 shows an example where the Q for the driven patch is fixed to $Q_a = 100$ and $Q_p = 15$ for the parasitic patch. Q_a has been considered larger than Q_p because the driven patch is placed closest to the groundplane. Fig. 14 shows the input impedance locus for the circuit model of Fig. 13 as a function of the coupling capacitor C_C. If the coupling increases (the parasitic patch is placed nearest of the driven patch) the input impedance shifts to a lower impedance and at the same time a locus appears. The size of the locus increases as the coupling increases. If the driven antenna feeding point has an impedance larger than 50 Ω [19], the locus can be placed at the center of the Smith chart resulting in an enhanced bandwidth (Fig. 15). Depending on the coupling between patches, the driven feeding point will be different. This feeding point condition is explained in detail in [19].

TABLE IV
BANDWIDTH IMPROVEMENT

	driven	stacked	
Sl[mm]	BW[%, $SWR = 2$]	BW[%, $SWR = 2$]	F
15	0.43	5.5	12.8
18	0.42	5.5	13

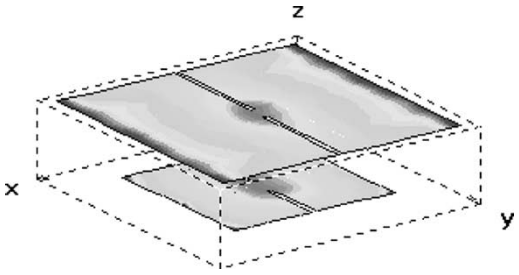

Fig. 20. Electrical current distribution.

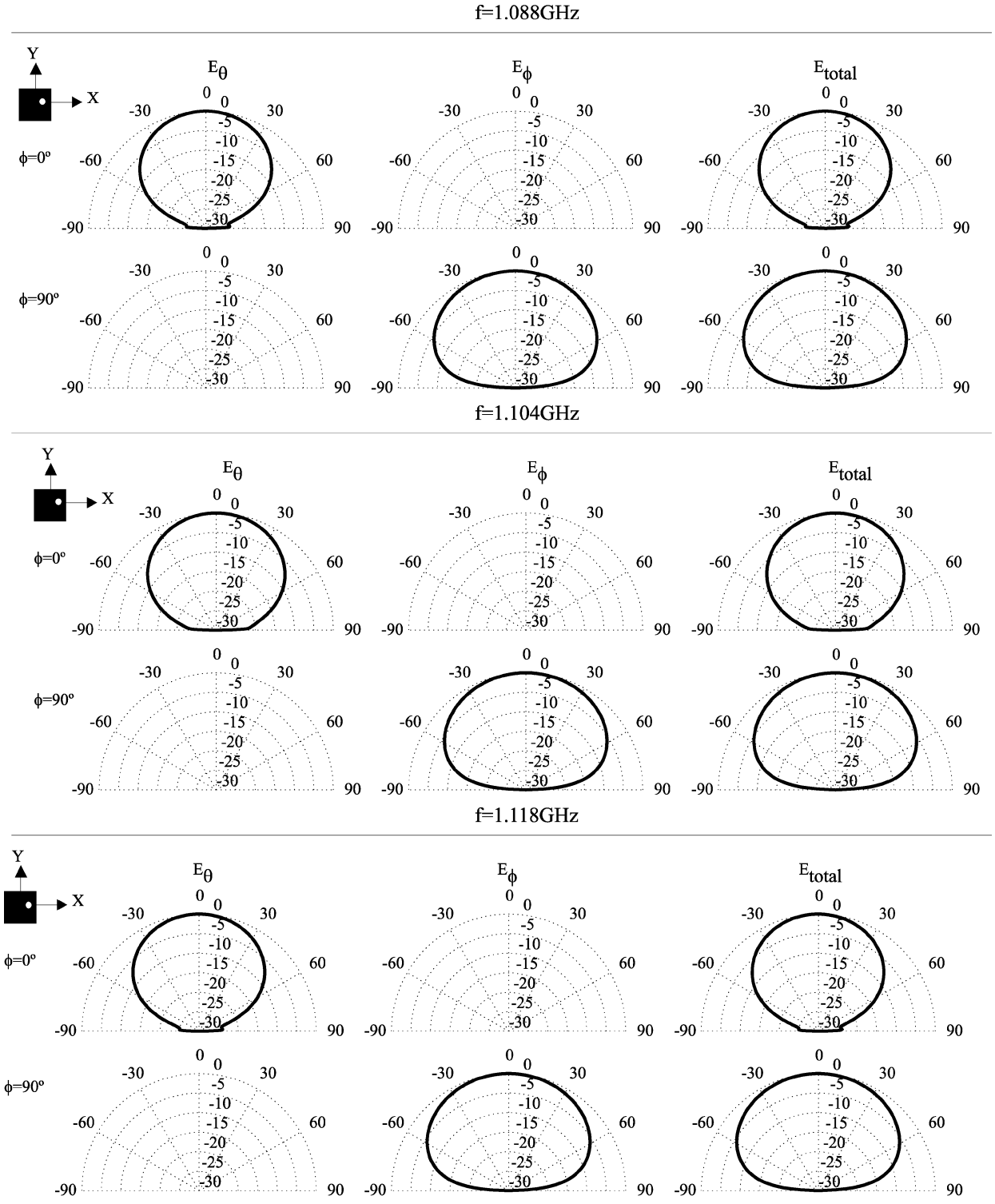

Fig. 21. Simulated main radiation cuts for $S_{LA} = 18$ mm prototype.

Fig. 15 shows an example of broadening the bandwidth of the single H-shaped MPA. The enhancing bandwidth factor F is a figure of merit relating the obtained bandwidth with the stacked structure divided by the bandwidth of the single H-shaped MPA. It is defined as follows:

$$F = \frac{BW_{\text{stacked-antenna}}}{BW_{\text{single-antenna}}}. \tag{15}$$

For the simulated case, the bandwidth of the stacked antenna for $SWR < 2$ is $BW_p = 8.4\%$ and for the single patch the bandwidth can be analytically calculated once the quality factor for the transmission line model loaded with the inductance is known. This quality factor results in $Q_a = 135$ so the $BW_a = 0.5\%$. With these values result $\mathrm{F} = 16.8$ which means than one can expect a broadening bandwidth factor around the theoretically calculated F.

Using such rule, several stacked H-shaped MPAs have been designed. In particular, the stacked technique has been applied for the $S_L = 15$ and 18 mm H-shaped MPA presented in the previous section. Dimensions of the prototypes are shown in Table III (see nomenclature of Fig. 1(b). For the $S_L = 18$ stacked antenna see extra slots in Fig. 17).

The parasitic patches are etched on the bottom part of the layer (fiber glass) represented in Fig. 1 with ε_{r3}. This way the dielectric material acts as supporting material for the parasitic patch and as a radome protecting the antenna. The dimensions of such dielectric is $80 \times 80\ \mathrm{mm}^2$ (Fig. 16).

In Fig. 17 are depicted the parasitic layouts for the measured prototypes. For the $S_{LA} = 18\ \mathrm{mm}$ two extra slots have been applied to match the parasitic resonant frequency with the resonant frequency of the driven patch and then the antenna can be matched.

The measured input impedance for the stacked patches is depicted in (Figs. 18 and 19) and is also compared with the single elements. Fig. 18 shows the measured input impedance locus for both stacked antennas. Note that the measured loops are very similar to the predictions (Fig. 14) obtained with the network model of Fig. 13.

Fig. 19 depicts the measured return loss for both stacked antennas as well as for the single elements of Section IV. It is significant to outline the broad bandwidth resulting when properly stacking a parasitic patch to the single driven patch.

To remark the bandwidth improvement, the figure of merit F is calculated (Table IV). The measured F is around 13 which is consistent with the theoretical predictions estimated with the electrical model which was 16.8 (Fig. 13).

The current distribution for the stacked $S_{LA} = 15\ \mathrm{mm}$ is depicted in Fig. 20. It is observed as the same TM mode distribution is presented in the driven and in parasitic patch.

The radiation patterns are then calculated to see how the directivity and efficiency has been improved (Fig. 21,Table V). Fig. 21 shows the computed radiation pattern for the stacked $S_{LA} = 18\ \mathrm{mm}$. Radiation pattern for the stacked $S_LA = 15\ \mathrm{mm}$ is very similar to the stacked $S_{LA} = 18\ \mathrm{mm}$.

Comparing Tables II and V it is observed that the directivity is increased about 2.5 dB for the stacked solution. On the other hand, the radiation efficiency has also increased dramatically, i.e., for the second stacked prototype is 86.7% while for the driven patch alone it was only 23%.

VI. Stacked H-Shaped MPA and the Limit of Chu

It has been shown that when the antennas becomes electrically smaller its bandwidth decreases. This bandwidth reduction of small antennas has been studied primarily by Chu [22] and Wheeler [23]. Chu derived an expression relating the antenna quality factor Q with the space the antenna fills: the radiansphere (Fig. 22). The diameter $(2a)$ of the radiansphere is the largest antenna dimension. Chu established a fundamental lossless Q limitatation given by

$$Q = \frac{1}{k^3 a^3} + \frac{1}{ka} \tag{16}$$

where $k = 2\pi/\lambda$, λ is the operating wavelength and a the radius of the radiansphere.

An antenna is said to be miniature if the radius $a < \lambda/2\pi$. Equation (16) is seen as a fundamental limit, that is, the limit

TABLE V
Directivity, Radiation Efficiency and Gain Simulations for the Stacked Antennas. Conductivity $\sigma = 4.9 \times 10^7\ \mathrm{S/m}$

Sl[mm]	D[dB]	η[%]	Gain[dB]
15	8.98	87.7	8.41
18	8.40	86.7	7.78

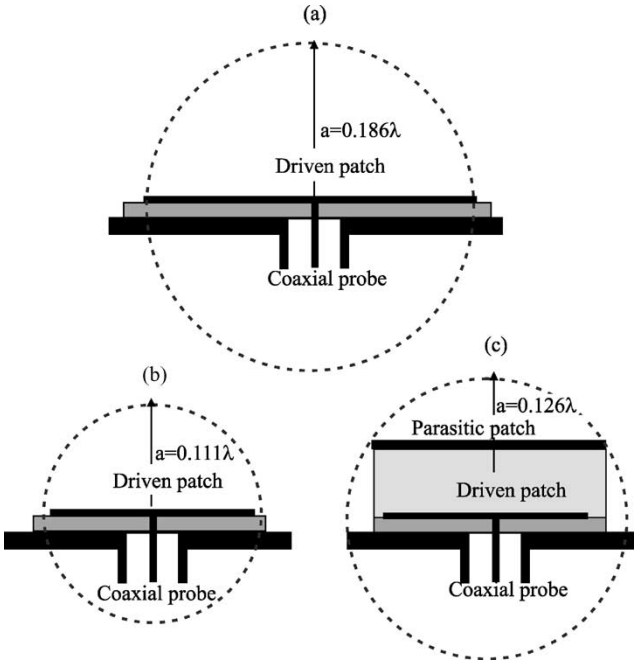

Fig. 22. Schema representing the radiansphere. a) Square MPA, b) driven $S_{LA} = 15\ \mathrm{mm}$, c) Stacked $S_{LA} = 15\ \mathrm{mm}$.

can never be exceeded. As commented is Section IV, if an antenna fills efficiently the radiansphere, its Q would be nearest to the limit of Chu. The dipole and MPAs does not fills properly the radiansphere, therefore, their Q is far from the limit of Chu and consequently are not effective as miniature antennas. The stacked H-shaped MPAs of Section V fill more efficiently the radiansphere so they are nearest from the Chu limit (Fig. 23).

Table VI shows the electrical size, the radius of the radiansphere and the Q. This values are plotted with respect the Chu's limit in Fig. 23. It can be observed from Fig. 23 that the square MPA can not be considered as a miniature antenna. The whole set of H-shaped MPA can be considered miniature antennas (the smallest single and stacked H-shaped MPA are presented). The single H-shaped MPA is far away to the limit of Chu when compared with its stacked version (one order of magnitude). This concludes that the stacked H-shaped MPA is a more efficient miniature antenna than the single H-shaped radiator having a similar $k \times a$ product.

VII. Conclusion

A transmission line model has been proposed to determine how the resonant frequency of the H-shaped patch can be reduced. On the other hand, the transmission line model has been also useful to model the input impedance behavior of the stacked antenna.

An analysis from the square to the slot length 18 mm H-shaped patch shows how the antenna can be miniaturized. The price one has to pay is the reduction of radiation efficiency

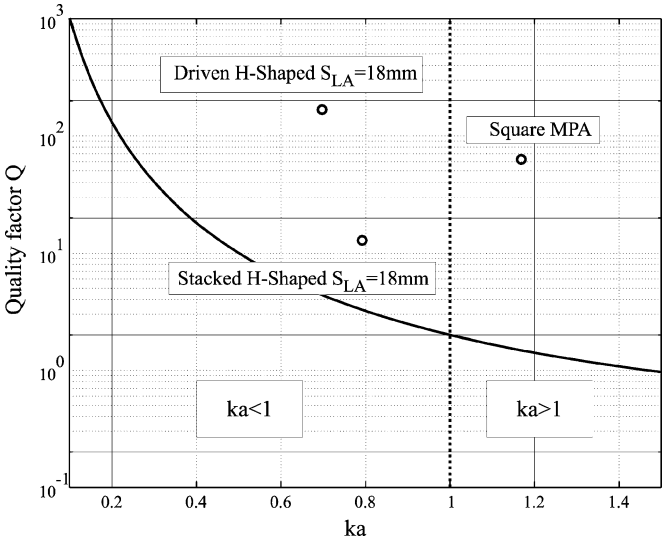

Fig. 23. Fundamental limit of the lossless Q versus the square, H-shaped $S_{LA} = 15$ mm and Stacked $S_{LA} = 15$ mm MPA.

TABLE VI
ELECTRICAL SIZE, RADIANSPHERE RADIUS AND Q. ES = Electrical Size

Antenna	ES[λ]	$a[\lambda]$	Q
Square	0.264	0.186	63
Driven $S_{LA} = 18$	0.158	0.111	168
Stacked $S_{LA} = 18$	0.178	0.126	12.8

and bandwidth. Directivity remains almost constant through all the perturbations.

To increase the poor radiation efficiency and bandwidth of the H-shaped MPA a stacked structure has been proposed. Results show that radiation efficiency can be increased from 23% to 87% and the bandwidth can be increased by a factor of 13. Directivity has also been raised by 2 dB.

The antennas under investigation has been discussed using the fundamental limit of Chu for electrically small antennas concluding that the stacked H-shaped MPA is more efficient than the single driven MPA.

REFERENCES

[1] D. M. Pozar and D. H. Schaubert, *Microstrip Antenna Design*. Piscataway, NJ: IEEE Press, 1995.

[2] R. Gonzalo, P. de Maagt, and M. Sorolla, "Enhanced patch-antenna performance by supressing surface waves using photonic-bandgap substrates," *IEEE Trans. Microwave Theory Tech.*, vol. 39, pp. 1513–1521, 1991.

[3] J. T. Aberle, D. A. Buchanan, and W. E. McKinzie, "Simulation of artificial magnetic materials using lattices of loaded molecules," in *Proc. Int. Symp. Optical Science, Engineering and Instrumentation*, 1999.

[4] L. Shafai, "Characterisitcs of printed ring antennas," in *Proc. Symp. Antenna Technol. Appl. Electromagn.*, vol. 96, Montreal, Canada, Aug. 1996, pp. 379–382.

[5] V. Palanisamy and R. Gary, "Rectangular ring and H shaped microstrip antennas- alternatives to rectangular patch antennas," *IEE Electron. Lett.*, vol. 21, no. 19, pp. 874–876, 1985.

[6] H. Y. Wang and M. J. Lancaster, "Aperture-coupled thin-film superconducting meander antennas," *IEEE Trans. Antennas Propagat.*, vol. 47, pp. 829–836, May 1999.

[7] J. Anguera, C. Puente, C. Borja, R. Montero, and J. Soler, "Small and high directivity bowtie patch antenna based on the sierpinski fractal," *Microwave Opt. Technol. Lett.*, Nov. 2001.

[8] C. Puente, E. Rozan, and J. Anguera, "Space Filling Miniature Antenna," Invention Patent PCT/EP00/00 411.

[9] R. B. Waterhouse, "Small microstrip patch antenna," *IEE Electron. Lett.*, vol. 31, no. 8, pp. 604–605, Apr. 1995.

[10] N. G. Alexopoulos and D. R. Jackson, "Fundamental superstrate cover effects on printed circuit antennas," *IEEE Trans. Antennas Propagat.*, vol. AP-32, pp. 807–816, 1984.

[11] D. Singh, C. Kalialakis, P. Gardner, and P. S. Hall, "Small H-shaped antennas for MMIC applications," *IEEE Trans. Antennas Propagat.*, vol. 48, pp. 1134–1141, July 2000.

[12] H. A. Wheeler, "Fundamental limitations on small antennas," *Proc. IRE*, pp. 1479–1488, Dec. 1947.

[13] H. Pues and A. Van de Capelle, "Accurate transmission-line model for the rectangular microstrip antenna," *Proc. Inst. Elect. Eng.: Microwave Antennas Propagat.*, pt. H, vol. 133, pp. 334–340, Dec. 1984.

[14] D. M. Pozar, *Microwave Engineering*, 2nd ed. New York: Wiley, 1998.

[15] K. C. Gupta, *Microstrip Lines and Slot Lines*, 2nd ed. Norwood, MA: Artech House, 1996.

[16] G. Kumar and K. C. Gupta, "Broadband microstrip antennas using additional resonators gap coupled to the radiating edges," *IEEE Trans. Antennas Propagat.*, vol. 32, pp. 1375–1379, 1985.

[17] ——, "Nonradiating edges and four edges gap coupled resonator broadband microstrip antennas," *IEEE Trans. Antennas Propagat.*, vol. 33, pp. 173–178, 1985.

[18] H. Chaloupka, N. Klein, M. Peiniger, H. Piel, A. Pischke, and G. Splitt, "Miniaturized high-temperature superconductor microstrip patch antenna," *IEEE Trans. Microwave Theory Tech.*, vol. 39, pp. 1513–1521, 1991.

[19] J. Anguera, C. Puente, and C. Borja, "A procedure to design stacked microstrip patch antenna based on a simple network mode," *Microwave Opt. Technol. Lett.*, Aug. 2001.

[20] F. Pues and R. Van De Capelle, "An impedance-matching technique for increasing the bandwidth of microstrip antenna," *IEEE Trans. Antennas Propagat.*, vol. 37, pp. 1345–1354, Nov. 1989.

[21] J. Anguera, C. Puente, C. Borja, G. Font, and J. Soler, "A systematic method to design single-patch broadband microstrip patch antennas," *Microwave Opt. Technol. Lett.*, Nov 2001.

[22] L. J. Chu, "Physical limitations of omnidirectional antennas," *J. Appl. Phys.*, vol. 19, pp. 1163–1175, Dec. 1948.

[23] H. A. Wheeler, "The radiansphere around s small antenna," *Proc. IRE*, pp. 1325–1331, Aug. 1959.

Jaume Anguera (S'99–M'03) was born in Vinaròs, Spain, in 1972. He received the Technical Ingeniero degree in electronic systems and Ingeniero degree in electronic engineering, both from the Ramon Llull University (URL), Barcelona, Spain, in 1994 and 1997, respectively, and the Ingeniero and Ph.D degrees in telecommunication engineering from the Polytechnic University of Catalonia (UPC), Barcelona, Spain, in 1998 and 2003, respectively.

From 1998 to 2000, he was a doctorate student with the Electromagnetic and Photonic Engineering Group (EEF), Signal Theory and Communications Department, UPC. In 1999, he was a Senior Researcher at Sistemas Radiantes, Madrid, Spain, where he was involved in the design of a dual-frequency dual-polarized fractal-shaped microstrip patch array for mobile communications systems. Also in 1999, he became an Assistant Professor at the Department of Signal Theory and Communications, Universitat Ramon Llull, where he is teaching antenna theory and preparing an e-learning antenna course. From 2000 until October 2003, he was with Fractus S.A., Barcelona, Spain, he is currently with Fractus-Korea where he holds the Research and Development Manager position. He is currently leading projects on fractal-shaped antennas for base station systems, working in the design of multiband monopoles, dual-polarized microcell antennas, microstrip patch arrays, feeding network architectures, broadband matching networks, high isolation techniques and array pattern synthesis with genetic algorithms. His current research interests are fractal, wideband, multiband, and high-directivity printed antennas. He holds 14 patents on fractal an other related antennas. He is author and coauthor of more than 50 journal, international and national conference papers and he has directed more than 24 Master's Thesis.

Dr. Anguera was a Member of the fractal team that in 1998 received the European Information Technology Grand Prize from the European Council for the Applied Science and Engineering and the European Commission for the fractal-shaped antenna application to cellular telephony. He was the finalist for the Best Doctoral Thesis 2003 ("Fractal and Broadband Techniques on Miniature, Multifrequency, and High-Directivity Microstrip Patch Antennas") on UMTS. This prize has been promoted by Technology Palns on UMTS promotion given by Telefónica Móviles España. He is one of the New Faces of Engineering 2004 (program supported by IEEE, IEEE Foundation, and National Engineers Weeks supporters). He was Session Chair for the 2003 International Symposium on Antennas and Propagation which was held in Columbus, OH. He was on the Scientific Committee of the 27th ESA Antenna Technology Workshop on Innovative Periodic Antennas, Santiago de Compostela, Spain, 2004.

Lluís Boada was born in Barcelona, Spain, in 1974. He received the Technical Ingeniero degree in communications systems from the Polytechnic University of Catalonia, Barcelona, Spain, in 2001.

From 2001 to 2003, he was an Assistant in the Communications Laboratory, Polytechnic University of Catalonia. Currently, he is with Fractus S.A., Barcelona, Spain, where he is responsible for the RF Laboratory and is involved in the design of mobile and base station

Carles Puente (S'91–M'93) was born in Badalona, Spain, in 1968. He received the Ingeniero degree in telecommunications engineering from the Polytechnic University of Catalonia (UPC), Barcelona, in 1992, the M.S. degree from the University of Illinois at Urbana-Champaign (UIUC) in 1994, and the Ph.D. degree from the UPC in 1997.

From 1994 to 1999, he was with the faculty of the Electromagnetics and Photonics Engineering group (EEF), UPC, and worked there in lidar systems and in the development of the fractal technology applied to antennas and microwave devices. He is one of the Founders of Fractus S.A., Barcelona, Spain, where since September 1999, he has been the Chief Technology Officer. He holds several patents on fractal and other related antenna and microwave inventions.

Dr. Puente was awarded the Best Doctoral Thesis in Mobile Communications in 1997 by the Colegio Oficial de Ingenieros de Telecomunicación (COIT) and ERICSSON, and in 1998 he and his team received the European Information Technology Grand Prize from the European Council for the Applied Science an Engineering (EuroCASE) and the European Comission, for his work in fractal-shaped antennas and their application to cellular telephony. He was awarded with the Premi Ciutat de Barcelona in 1999.

Carmen Borja (S'99–M'03) was born in Barcelona, Spain, in 1972. She received the Ingeniero degree in telecommunications engineering and the Ph.D. degree from the Polytechnic University of Catalonia (UPC), Barcelona, Spain, in 1997 and 2001, respectively.

From 1997 to 2000, she was with the Electromagnetics and Photonics Engineering group (EEF), UPC where she worked in the development of fractal technology applied to microstrip antennas. Since June 2000, she has been with Fractus S.A., Barcelona, Spain, where she holds the Project Manager position. During the summer of 1999, she was working in the Antenna, Research, Analysis, and Measurement Laboratory, University of California, Los Angeles (UCLA). She holds several patents on fractal and other antenna inventions. She has authored and co-authored over 25 technical journals and conferences papers from the IEEE and IEE. She has been the director of several Master Thesis at the UPC. Her research interests are fractal, miniature and multi-band antennas.

Dr. Borja was awarded with the Best Doctoral Thesis in Advanced Mobile Communications 2002 by the Colegio Oficial de Ingenieros de Telecomunicación (COIT) and Fundación Airtel-Vodafone. In 1998, the team where she worked at the UPC received the European Information Technology Grand Prize from the European Council for the Applied Science and Engineering (EuroCASE) and the European Commission, for the work in fractal-shaped antennas and their application to cellular telephony.

Jordi Soler (S'99–M'03) was born in Mataró, Spain, in 1975. He received the Technical Ingeniero and Ingeniero degrees in telecommunication engineering, both from the Politechnic University of Catalonia (UPC), Barcelona, Spain, in 1996 and 1999, respectively, where he is working toward the Ph.D. degree in multiband and wideband small fractal-shaped antennas.

In 1996, he joined the Electromagnetics and Photonics Engineering Group (EEF), Signal Theory Communications Department (TSC), UPC, to collaborate in a project related to laser remote sensing (LIDAR), where from 1997 to 1999, he worked in the TSC Department as a radiofrequency laboratory technician, where he was mainly engaged in near and far field antenna measurements. Since June 2000, he has been working at Fractus, S.A., Barcelona, Spain, as a Project Manager leading projects related to the automotive market, indoor antennas, antennas for handsets, and defense projects. He is author and coauthor of more than 15 papers published in magazines, journals and international and national antenna conferences. He holds several patents on fractal and other related antenna inventions.

Mr. Soler received the Best Engineer Degree Final Project Award on New Technologies Applied to Antennas and Radiating Systems by the Spanish College of Telecommunication Engineers (COIT) and RYMSA in 1999. He received the Best AP2000 Poster Paper Award on Antennas in the AP2000 Millennium Conference on Antennas and Propagation, which was held in Davos, Switzerland, April 2000. He was invited to act as Session Chair in the 2000 International Symposium on Antennas and Propagation, Fukuoka, Japan, August 2000. He also was Session Chair at the 2002 International Symposium on Antennas and Propagation, San Antonio, TX, July 2002.